Journal of Computational Science &Engineering 40 (2019) 1046-1050

Available at http://www.asocse.org ISSN 1710-4068

NOx sensing on pure and Al doped g-C_3N_4 surfaces

Zhenze Liu[1], Yuan Liang[2], Juan Feng[1], Fenghui Tian[1,*]

[1]Institute of Computational Science and Engineering, State Key Laboratory of Bio-Fibers and Eco-Textiles, College of Environmental Science and Engineering, Qingdao University, Qingdao, 266071, China

[2]Key Laboratory of Low Carbon Energy and Chemical Engineering, College of Chemical and Environmental Engineering, Shandong University of Science and Technology, Qingdao, 277590, China

Abstract: **In this work, we studied pure and Al doped graphitic carbon nitride (g-C_3N_4) for NOx sensing using density functional theory (DFT) calculations. The calculation results show that pure g-C_3N_4 can achieve high-efficiency sensing of NO and NO_2, and the charge transfer amounts are 0.291e and 0.226e, respectively. NO2 adsorbed to the surface of Al-doped g- C_3N_4, chemical adsorption occurs, and Al-O bonds were formed with Al atoms. The charge transfer reaches 0.469e, and the sensing effect is doubled. Therefore, pure g- C_3N_4 can achieve high-efficiency sensing for both NO and NO_2, while Al-doped g- C_3N_4 is a promising material for NO_2 ultra-high sensing.**

Keywords: NOx sensing; g-C_3N_4 surface; Al doped; Density functional theory

Received 7 March 2019, Revised 8 April 2019, Accepted 10 April 2019

*Corresponding Author: Fenghui Tian, Leo950118@163.com

1. Introduction

As one of the main pollutants of air pollution, nitrogen oxides (NOx) mainly come from automobile exhaust emissions and other combustion equipment[1,2]. In the usual sense, nitrogen oxides (NOx) refer to NO and NO_2. Excessive NOx emissions not only pollute the atmosphere, but also cause acid rain, global warming and photochemical smog[3.4], which can also cause lung and respiratory diseases in humans[5]. Therefore, there is an urgent need to develop high-performance gas sensing materials to monitor and detect NOx generated in various production and life.

Recently, the performance of graphene-like material g-C_3N_4 in the gas sensing direction has attracted people's attention. g-C_3N_4 is a single-layer nanostructure of sp2 hybridized carbonized nitrogen with a band gap of 2.7 eV[6], and its physicochemical properties are stable, non-toxic and easy to prepare[7-9]. Graphene with a representative two-dimensional material has a lower sensitivity to gas[10-13], and the g-C_3N_4 sensor prepared by Donghong Wang[14] has good sensitivity to NO2 and has high selectivity. In the study of Zhu et al., it was found that Os doping can significantly increase the adsorption of NO by g-C_3N_4[15]. However, there is currently no comprehensive study of the effects of g-C_3N_4 on NOx sensing and doping. Therefore, the sensing of NOx by g-C_3N_4 and the effect of doping on sensing are very worthy of discussion.

In this work, we studied the adsorption and sensing behavior of NO and NO_2 on the pure and Al-doped g-C_3N_4 by density functional theory. It is found that NO_2 is adsorbed on the hole2 site in parallel, and the charge transfer amount is 0.215e. NO gas molecule also likes to adsorb on the $hole_2$ site, and the charge transfer is 0.291e. After Al doping, the sensing effect of NO_2 is greatly improved, and the charge transfer amount is increased to 0.469e. In general, g-C_3N_4 is a good NOx sensing material, and Al doping can greatly improve the sensitivity of g-C_3N_4 to NO_2.

2. Computational details

The calculations have been performed by using the Doml[3] package in Material Studio[16]. The generalized gradient approximation utilizing the functional of Perdew-Bruke-Ernzerhof (PBE) was employed[17]. The double-numerical-quality basis set with polarization functions (DNP) was adopted to describe the valence orbital of the atoms. The core electrons were substituted by DFT semi-core pseudopotentials (DSPPs)[18]. A vacuum region of 10 Å was employed to avoid interactions between layers. The Monkhorst−Pack K-point was set as 2 × 2 × 1. The energy, force, and displacement convergence criteria were set to 2.0 × 10−5 Hartree, 4.0 × 10−3 Hartree/Å, and 5.0 × 10−3 Å, respectively.

The Eads for adsorption of gas molecule over the pristine and Al−doped g-C_3N_4 systems were defined as Eads = E(G/g-C_3N_4) − E(g-C_3N_4) − E(G), where $E(G)$ is the energy of a free gas molecule, E(g-C_3N_4) is the energy of the g-C3N4 surface slab, and E(G/g-C_3N_4) is the total energy of the surface with gas molecule adsorption. According to this equation, a positive value of Eads indicates a favourable adsorption system.

3. Results and discussions

2019@ The American Computational Science Society. All rights reserved.

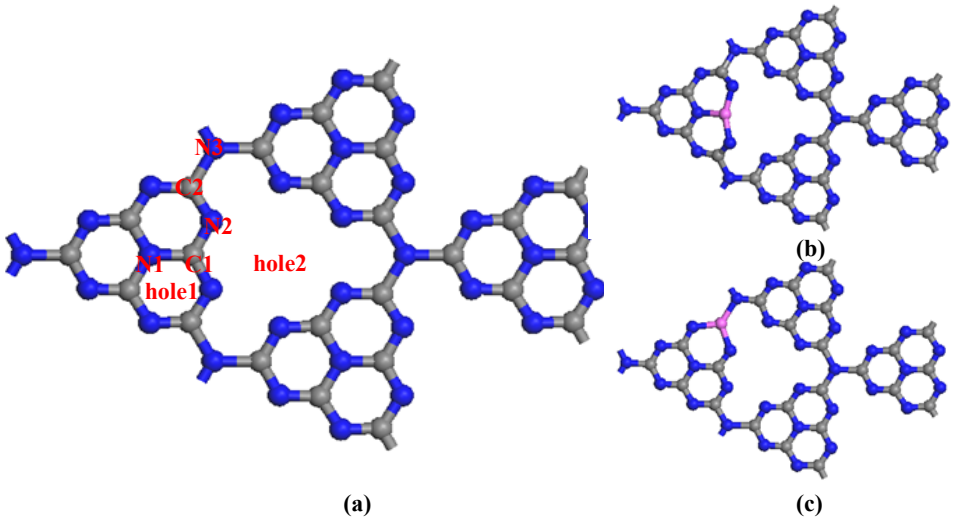

Figure 1. Optimized structure: (a) pure g-C_3N_4 (b) Al doped g-C_3N_4 at C_1 active site. (c) Al doped g-C3N4 at C_2 active site. The blue, gray, and pink spheres are the N, C, and Al atoms, respectively.

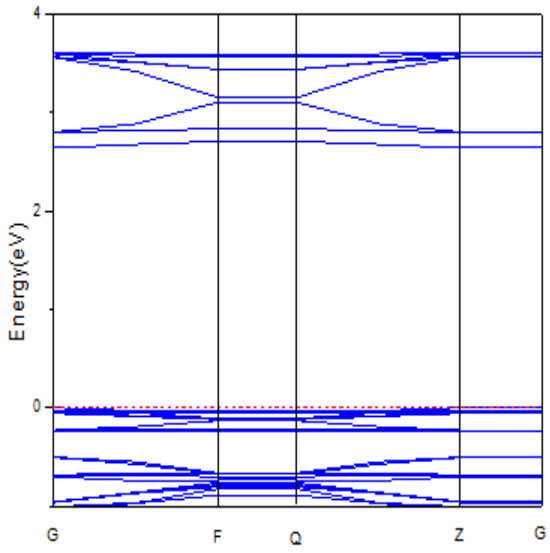

Figure 2. Energy band structure of g-C_3N_4.

3.1. NO adsorption on pure g-C_3N_4 surface

Figure 2.(a) shows an optimized structure of g-C_3N_4 containing 24 C atoms and 32 N atoms. N atoms can be classified into three types, namely two tricoordinates and one double-coordinate N atom, labeled N_1, N_3 and N_2, respectively. C atoms can be divided into two types, the label near the N_1 atom is C_1, and the label near the N_2 atom is C_2. A hexagonal aperture consisting of 3 C atoms and 3 N atoms is labeled as $hole_1$. A large triangular hole composed of 9 N atoms and 9 C atoms is labeled as $hole_2$. We used the Al atom to dope the two C atoms on g-C3N4, which are denoted as Figure 2 (b) Al_1 and Figure 2 (c) Al_2, respectively. The energy band structure of g-C_3N_4 is shown in Figure 2. It shows that g-C3N4 is a direct bandgap semiconductor. The calculated band gap is 2.64 eV, which is consistent with the experimental value of 2.7 eV [19].

First, we studied the adsorption sensing of NO on the surface of g-C_3N_4. In the calculation, we placed the NO gas molecules on the surface of g-C_3N_4 in both parallel and vertical directions with an initial distance of 3 Å. The optimized N-O bond length is 1.154A. We found that only NO adsorbed at the hole2 active site, and there was a charge transfer of up to 0.291e, enabling efficient sensing. While the charge transfer of d at other adsorption sites is less than the minimum value of effective detection of 0.070 e[20] or 0.080 e[21], effective sensing cannot be achieved.

Table1. Adsorption energies and Charge transfer for NO adsorbed on g-C_3N_4 surface

Confgurations	Ead(eV)	Charge Transfer(e)
C1-V	0.10	0.045
C1-P	0.03	0.052
C2-V	0.01	0.052
C2-P	0.03	0.056
hole1-V	0.07	0.042
hole1-P	0.02	0.047
hole2-V	**0.31**	**0.291**
hole2-P	0.09	0.105
N1-V	0.03	0.031
N1-P	0.06	0.040
N2-V	0.10	0.056
N2-P	0.01	0.062
N3-V	0.01	0.054
N3-P	0.02	0.061

2019@ The American Computational Science Society. All rights reserved.

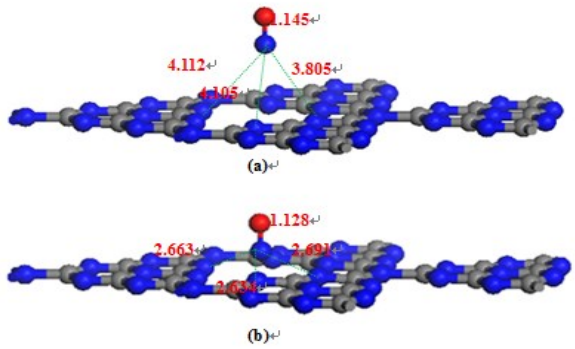

Figure 3. Adsorption confgurations of hole2-V on g-C3N4 surface: (a) Initial confguration. (b) Optimized configuration.

We use hole$_2$-V as an example to explore the sensing mechanism of g-C_3N_4 for NO. Figure 3 is a comparison of the model before and after hole$_2$-V adsorption. We found that the NO moves vertically downward after adsorption and is attracted to the surface of g-C_3N_4. The distance of the N-O bond was shortened from 1.154 Å to 1.128 Å, and the surface of g-C_3N_4 was not significantly deformed, and the adsorption energy of the hole2-V model was 0.31 eV. These phenomena indicate that the adsorption is physical adsorption. The hole$_2$ on the surface of g-C_3N_4 has a large adsorption capacity for NO, and electrons are transferred from NO to the surface, and NO is oxidized. This should be the reason why the surface of g-C3N4 material can achieve high-efficiency sensing of NO.

3.2. NO_2 adsorption on g-C_3N_4 surface

Table 2. Adsorption energies and Charge transfer for NO_2 adsorbed on g-C_3N_4 surface

Confguratio ns	Ead(eV)	Charge Transfer(e)
C_1-V	0.17	-0.18
C_1-P	0.16	-0.173
C_2-V	0.16	-0.173
C_2-P	0.28	-0.204
hole$_1$-V	0.23	-0.192
hole$_1$-P	0.26	-0.215
hole$_2$-V	0.09	-0.137
hole$_2$-P	0.20	-0.139
N_1-V	0.21	-0.198
N_1-P	**0.27**	**-0.226**
N_2-V	0.17	-0.170
N_2-P	0.30	-0.188
N_3-V	0.18	-0.164
N_3-P	0.20	-0.193

Next, we studied the adsorption sensing of NO_2 on the surface of g-C_3N_4.Similarly, we placed the NO_2 gas molecules on the g-C_3N_4 surface in both parallel and vertical directions with an initial distance of 3 Å.The optimized NO_2 molecule has an N-O bond length of 1.200 Å and an O-N-O angle of 133.439°. Compared with NO, NO can only be adsorbed on the active site of hole$_2$ to achieve sensing. NO_2 can achieve effective sensing on the so-called site adsorbed on the surface of g-C_3N_4[20-21], and even efficient sensing. After optimization, we found that most of the parallel adsorption configurations have more charge transfer and higher adsorption energy than their corresponding vertical adsorption configurations by the amount of charge transfer and the amount of adsorption energy. Therefore, parallel adsorption is the dominant adsorption configuration of NO_2 on the surface of g-C_3N_4, and NO_2 can achieve high-efficiency sensing on the surface of g-C_3N_4.

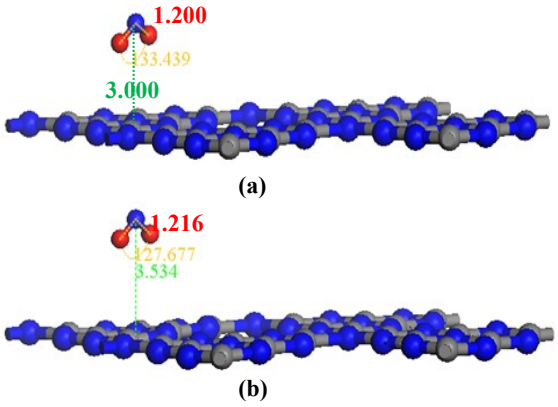

Figure 4. Adsorption confgurations of N_1-P on g-C_3N_4 surface: (a) Initial confguration. (b) Optimized configuration.

Taking the N_1-P adsorption model with the largest charge transfer (Figure 4) as an example, we explored the sensing mechanism of NO_2 on the surface of g-C_3N_4. Before optimization, the NO_2 molecule was placed above the surface 3 Å. After optimization, the NO_2 molecule was pushed farther to the surface 3.534 Å. The N-O bond length is extended from the original 1.200 Å to 1.216 Å. The O-N-O key was reduced from the original 133.439° to 127.677°. From these macroscopic physical properties and the adsorption energy of 0.27 eV, it is known that NO_2 adsorption is a physical adsorption in g-C_3N_4. To investigate the sensitivity of g-C_3N_4 to NO_2 gas, we further analyzed the Mulliken charge layout of the N_1-P model. According to Mulliken's charge distribution analysis, the NO_2 molecule is electrically neutral before adsorption. After adsorption, the Mulincan charges of two O atoms and one N atom are -0.275, -0.277 and 0.326e, respectively. This indicates that two oxygen atoms obtained 0.552e from the surface, while the N

2019@ The American Computational Science Society. All rights reserved.

atom lost 0.326e, and the entire NO_2 gave 0.226e, showing strong oxidizability. Therefore, we suspect that the strong oxidative properties of NO_2 molecules should be the main reason for efficient sensing on the surface of g-C_3N_4.

Table 3. Mulliken population analysis of the N_1-P Configuration

Systems	Confgurations	Atom	Before adsorption/e	After adsorption/e	Charge transfer/e
g-C_3N_4	N1-P	O	0	-0.275	-0.226
		N	0	0.326	
		O	0	-0.277	

3.3. NO and NO_2 adsorption on Al doped g-C_3N_4 surface

Finally, we explored the adsorption sensing of NO and NO_2 on the surface of Al-doped g-C_3N_4. For NO, Al doped does not improve the sensing effect of NO, but is disadvantageous for NO sensing. The amount of charge transfer was reduced from 0.291e to 0.100e. However, the doped of Al is advantageous for the adsorption of NO, and the adsorption energy is increased from 0.31 eV to 1.24 eV. For NO_2, Al doped can greatly improve its sensing. After Al doped, the adsorption energy increases sharply from 0.27 eV to 3.55 eV, and the charge transfer amount increases from 0.226e to 0.469e. It can be concluded that Al doping can achieve super-sensing of g-C_3N_4.

Table 4. Adsorption energies and Charge transfer for NO and NO_2 adsorbed on Al doped g-C_3N_4 surface

Systems	Confgurations	Ead(eV)	Charge Transfer (e)
NO	Al_1-NO-V	0.08	-0.08
	Al_1-NO-P	0.49	-0.100
	Al_1-ON-V	0.52	-0.07
	Al_2-NO-V	0.84	-0.09
	Al_2-NO-P	1.14	-0.100
	Al_2-ON-V	1.24	-0.09
NO2	Al_1-NO_2-V	1.62	-0.402
	Al_1-NO_2-P	1.62	-0.430
	Al_2-NO_2-V	2.40	-0.421
	Al_2-NO_2-P	3.55	-0.469

We have investigated the reasons why Al doping can greatly improve the sensing effect of g-C_3N_4 on NO_2. The model of Al_2-NO_2-P is shown in Figure 5. The initial parallel placement is at a distance of 3 Å from the surface. After optimization, the molecules are pulled closer to the surface. The distance between the two oxygen atoms and the surface-doped Al atoms is 1.925 Å and 1.931 Å, this has generated two Al-O bonds and chemical adsorption has taken place. It can be seen from the charge density diagram that the two oxygen atoms of the NO_2 molecule and the surface-doped aluminum atoms do form two Al-O bonds. NO_2 adsorbs to the surface of Al-doped g-C_3N_4 andthen forms Al-O bond with Al atom, which causes chemisorption. This is why Al doping can improve the NO_2 sensing of g-C_3N_4.

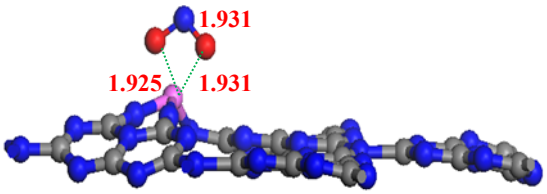

Figure 5. The Al2-NO2-P confguration after optimization.

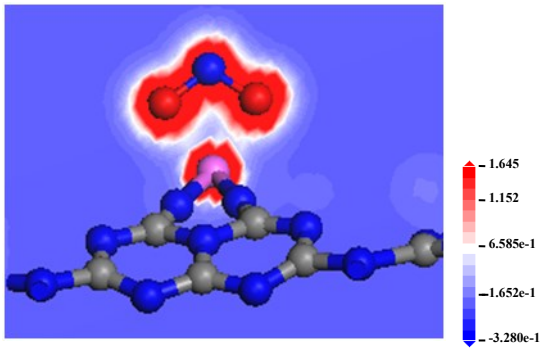

Figure 6. The electron density of Al_2-NO_2-P confguration.

4. Conclusion

In this paper, the adsorption sensing behavior of NO and NO_2 on the surface of pure and Al-doped g-C_3N_4 was detected by DFT calculation. It was found that pure g-C_3N_4 can achieve high-efficiency sensing of NO and NO_2, and the charge transfer amounts are 0.291e and 0.226e, respectively. When we implemented Al

2019@ The American Computational Science Society. All rights reserved.

doping on g-C_3N_4, we found that it had a two-fold increase in the sensing of NO_2, and the charge transfer amount reached an astonishing 0.469e. In general, pure g-C_3N_4 can achieve high-efficiency sensing for NO and NO_2, while Al-doped g-C_3N_4 is a promising material for NO_2 ultra-high sensitivity sensing.

References

[1] K. Skalska, J.S. Miller, S. Ledakowicz. Sci., Total Environ. 408 (2010) 3976–3989.
[2] B. Chen, C. Hong, H. Kan. Toxicology, 198 (2004) 291–300.
[3] B. Zhao, S.X. Wang, H. Liu, et al. Atmos. Chem. Phys., 13 (2013) 9869–9897.
[4] H. He, Y.S. Wang, et al. Scientific Reports, 4 (2014) 4172.
[5] A.M. Andringa, C. Piliego, I. Katsouras, P.W.M. Blom, D.M. de Leeuw. Chem. Mater., 26 (2014) 773–785.
[6] G. Dong, L. Yang, F. Wang. ACS Catal. 6 (2016) 6511−6519.
[7] Y. Wang, X.C. Wang, M. Antonietti. Angew. Chem. Int. Ed., 51 (2012) 68.
[8] Y. Zheng, J. Liu, J. Liang, M. Jaroniec, S.Z. Qiao. Energy Environ. Sci, 5 (2012) 6717–6731.
[9] X.C. Wang, S. Blechert, M. Antonietti. ACS Catal, 2 (2012) 1596-1606.
[10] Leenaerts, B. Partoens, F. Peeters. Phys. Rev. B, 77 (2008) 125416.
[11] Y.H. Zhang, Y.B. Chen, K.G. Zhou. Nanotechnology 20 (2009) 185504.
[12] J. Dai, J. Yuan, P. Giannozzi. Appl. Phys. Lett., 95 (2009) 232105.
[13] S.M. Aghaei, M.M. Monshi I. Torres. S.M. Zeidi, I. Calizo. Applied Surface Science 427 (2018) 326–333
[14] D. Wang, W. Gu, Y. Zhang. RSC Adv, 4 (2014) 18003–18006.
[15] B. Zhu, S. Wageha. Catal. Today (2008).
[16] B. Delley. J. Chem. Phys. 113 (2000) 7756–7764.
[17] J.P. Perdew, K. Burke, M. Ernzerhof. Phys. Rev. Lett. 77 (1996) 3865–3868.
[18] B. Delley. Phys. Rev. B, 66 (2002) (1098-0121)
[19] N. Yang, G. Li, W. Wang. Journal of Physics and Chemistry of Solids, 72 (2011) 1319–1324.
[20] Y.B. Xue, Z.A. Tang. Sens. Actuators B, 138 (2009) 108–112.
[21] M. Hu, W.D. Wang, P. Zeng. Chin. Phys. B, 21 (2012) 023101–023107.

2019@ The American Computational Science Society. All rights reserved.